Dual-Mode Stepped-Impedance Ring Resonator for Bandpass Filter Applications

Michiaki Matsuo, Hiroyuki Yabuki, and Mitsuo Makimoto, *Senior Member, IEEE*

***Abstract*—It is well known that two orthogonal resonant modes exist within a one-wavelength ring resonator. In this paper, we focus on a ring resonator possessing an impedance step as a form of perturbation. A convenient analyzing method for obtaining the resonance characteristics of this resonator structure is presented. Furthermore, generation of attenuation poles obtained by the dual-mode ring resonator is discussed. In addition, a filter design method based on this resonator is explained, followed by experimental results, which prove the validity of the proposed design method.**

***Index Terms*—Attenuation poles, dual-mode filters, microstrip filters, ring resonators.**

I. Introduction

BANDPASS filters used for wireless telecommunication equipment require small size in addition to low loss. Miniaturization of the resonator is indispensable for a compact filter, and techniques such as the use of high-permittivity materials, variation of resonator structure, and use of multiple resonant modes are chiefly applied. The use of high-permittivity materials can effectively shrink the resonator by a factor of $1/\sqrt{\varepsilon_r}$, where ε_r is the relative dielectric constant of the dielectric material filling the resonator structure. Common ceramic material possess a relative dielectric constant of 30$\sim$100. A method of reducing the length of a transmission-line resonator by changing its characteristic impedance in a step manner is well known [1], [2], and this method is applied to dielectric coaxial resonators used for bandpass filters (BPFs) and diplexers of cellular phones [3]. The third method is the effective use of multiple resonant modes existing within a resonator structure; an approach mainly applied to three-dimensional resonator structures such as dielectric resonators and cavity resonators [4]–[6]. BPF designs, based on the dual resonant modes existing in planar-type resonators such as one-wavelength ring resonators and disk resonators, have also been reported [7], [8]. By utilizing such multiple modes, a multistage filter can be composed by fewer resonators than the number of stages.

The ring resonator is considered a standard resonator structure for the evaluation of strip-line configurations and dielectric substrate materials. Features such as its ease of design, excellent unloaded Q values due to low radiation loss, and no need of grounding qualify it as a suitable resonator structure for filters applied to microwave and millimeter-wave integrated circuits (ICs). While its large physical size stand a drawback, the use of its dual mode is considered promising for filter applications [9], [10]. Although some BPF configurations based on a ring-resonator structure have been reported, no analytical study has been carried out on the resonance characteristic and the coupling between the orthogonal modes that are needed for filter design.

Manuscript received April 18, 2000.

The authors are with the Mobile Communication Research Laboratory, Matsushita Research Institute Tokyo Inc., Kawasaki 214-8501, Japan.

Publisher Item Identifier S 0018-9480(01)05049-9.

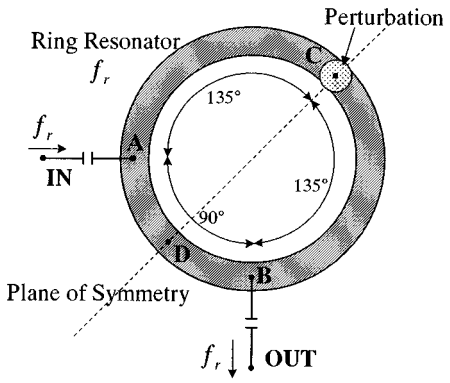

Fig. 1. Structure of dual-mode resonator based on a one-wavelength ring resonator.

Focusing on a ring resonator possessing an impedance step as a form of perturbation, in this paper, we present a convenient analyzing method for obtaining the resonance characteristics of the two orthogonal resonance modes and the coupling of these modes. At the same time, the attenuation poles caused by this configuration are discussed. Furthermore, the design method of a two-stage BPF based on this ring resonator is presented, followed by experimental results, which prove the validity of this design method.

II. Dual-Mode Ring Resonator

A. Structure

Fig. 1 shows the basic structure of a dual-mode ring resonator. The ring resonator is composed by connecting the two ends of a one-wavelength transmission line in a ring-like formation. Input and output ports are spatially separated at 90° in electrical length, and a perturbation is introduced within the resonator at a symmetrical location (Points C or D) 135° apart from both input and output ports. Without this perturbation, output port generates no response even when input port is excited at resonance frequency. The coupling between the two orthogonal modes is accomplished by introducing the perturbation within the resonator. General conditions to form a dual-mode resonator are as follows.

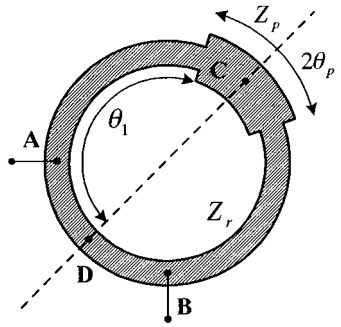

Fig. 2. Structure of dual-mode filter applying an impedance step as perturbation.

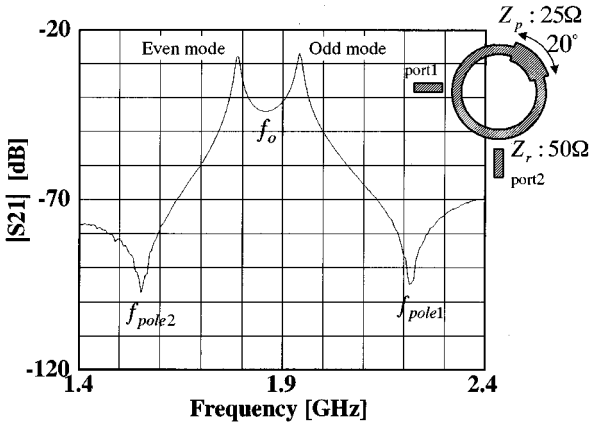

Fig. 3. Example of resonance characteristic of the experimental stepped-impedance-type dual-mode resonator.

1) The input and output ports should be spatially separated at 90°.
2) A discontinuity or some means of generating a reflected wave against an incident wave should exist within the ring resonator.
3) A plane of symmetry should exist in the circuit geometry.

Fig. 2 shows a dual-mode resonator realized by changing the characteristic impedance of the ring-resonator transmission line in a step manner at a certain position. The coupling strength between the orthogonal resonant modes can be controlled by both the impedance ratio and the length of the stepped transmission line.

B. Analysis Method of Resonance Characteristics

An example of the resonance characteristics of a dual-mode ring resonator is shown in Fig. 3. Typical resonance characteristics possess two resonance frequencies accompanied by attenuation poles on both sides. Here, we present the analysis method for obtaining the resonance frequencies and attenuation-pole frequencies.

1) Resonance Frequency: The symmetrical geometry of the ring-type dual-mode resonator allows us to explain its resonance operation by even- and odd-mode analysis [11]. The two resonance frequencies correspond to the resonance frequencies of each mode and are derived from equivalent circuits of each mode. For an even mode, the circuit is divided into one-half at the symmetrical plane, where it is open circuited. Conversely,

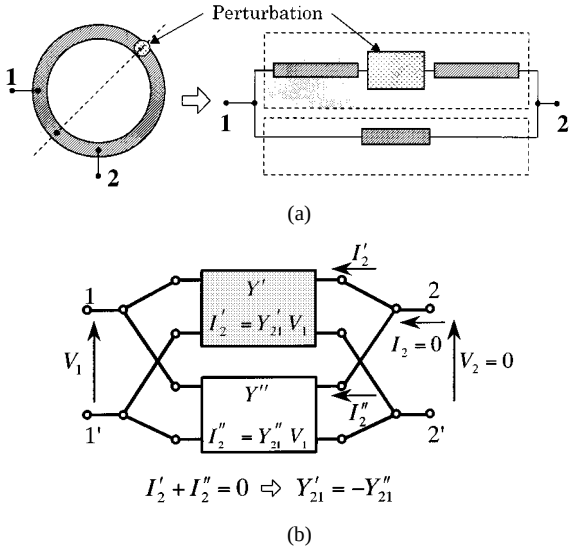

Fig. 4. Analysis method for obtaining attenuation poles of a dual-mode ring resonator. (a) Equivalent expression with two propagation paths. (b) Corresponding circuit expression using Y-matrices.

for an odd-mode excitation, this symmetrical plane is short circuited. For a simple ring resonator without any perturbation, the equivalent circuits of both the even- and odd-modes become a half-wavelength resonator and, hence, their resonance frequencies are identical. In this case, the orthogonal resonant modes in the ring resonator do not couple each other.

2) Attenuation-Pole Frequency: The dual-mode ring resonator features two attenuation poles that appear near the resonance frequency. This is because there exists two propagation paths between the input and output ports. This feature becomes highly effective for obtaining excellent attenuation characteristics near the passband when composing filters based on this resonator structure. In the case of a symmetrical circuit such as the dual-mode resonator, the attenuation pole exists at a frequency where the eigenimpedances of the even and odd modes are equal because the currents on the output side cancel each other.

The attenuation-pole frequency can be analyzed in the following manner. In the ring resonator in Fig. 4(a), let the Y-parameter of the two propagation paths connecting the input and output be Y' and Y'', respectively. The ring resonator is then equivalent to the parallel connection of these two circuits, as illustrated in Fig. 4(b). At an attenuation-pole frequency, the output voltage becomes zero ($V_2 = 0$) because the signal does not appear at output port 2 when input port 1 is excited. Therefore, the input voltage V_1 and the output currents I_2' and I_2'' are related only via parameter Y_{21} of each circuit. Since the output current I_2 is also zero, the condition can be introduced. Hence, the attenuation-pole frequencies can be calculated from (1) as follows:

$$Y_{21}' = -Y_{21}''. \tag{1}$$

Next, we present the analysis method giving the coupling coefficient between the orthogonal modes and the attenuation-pole frequencies for the impedance step configuration shown in Fig. 2, followed by experimental results to verify these results. Fig. 5 shows the even- and odd-mode equivalent

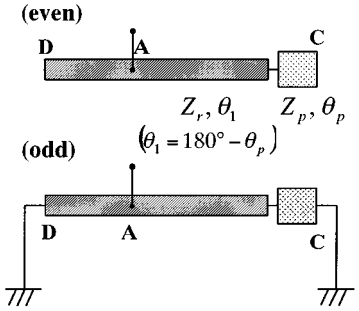

Fig. 5. Equivalent circuits of the stepped-impedance-type dual-mode ring resonator.

circuits of the impedance-step-type dual-mode resonator. Let Z_r and Z_p be the characteristic impedance of the ring transmission line and the perturbed portion. The equivalent circuits for both modes are a cascaded connection of transmission lines with a characteristic impedance of Z_r and Z_p. For a ring resonator without any perturbation, the total electrical lengths is 180° at resonance frequency f_r. In Fig. 2, when the electrical length of the perturbation is $2\theta_p$, the electrical length from Point D to the impedance step point is θ_1, and the characteristic impedance ratio is K_z ($K_z = Z_p/Z_r$), the resonance frequencies and attenuation poles can be derived from (2)–(4). Condition (4) applies to a perturbation at Point C. Here, the electrical length from Point A (or B) to the step is indicated as θ_2 ($\theta_2 = \theta_1 - 45°$).

(Even-mode resonance frequency: f_{0e})

$$K_z \tan(\theta_1 f'_{0e}) + \tan(\theta_p f'_{0e}) = 0$$
$$f'_{0e} = f_{0e}/f_r. \tag{2}$$

(Odd-mode resonance frequency: f_{0o})

$$\tan(\theta_1 f'_{0o}) + K_z \tan(\theta_p f'_{0o}) = 0$$
$$f'_{0o} = f_{0o}/f_r. \tag{3}$$

(Attenuation-pole frequencies: f_{pole})

$$\sin(2\theta_p f'_p)\left\{K_z \cos^2(\theta_2 f'_p) + \frac{1}{K_z}\sin^2(\theta_2 f'_p)\right\} + \sin(2\theta_2 f'_p)\cos(2\theta_p f'_p) + \sin\left(\frac{\pi}{2} f'_p\right) = 0$$
$$f'_p = f_{\text{pole}}/f_r. \tag{4}$$

Fig. 6 illustrates resonance characteristics in relation to the perturbation length. Here, impedance ratio K_z is considered a constant of 0.5. The frequencies indicated in Fig. 6 are normalized by resonance frequency f_r. Results imply that, the longer the perturbed portion, the stronger the coupling between orthogonal modes becomes. However, the center of the two resonance frequencies changes little in relation to perturbation length. When the perturbation is loaded at Points C or D of

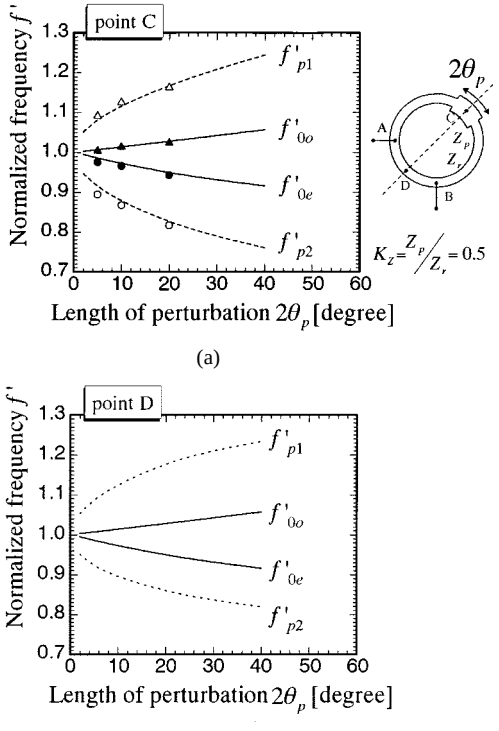

Fig. 6. Resonance characteristics of the stepped-impedance-type dual-mode ring resonator as a function of step length $2\theta_s$. (a) Perturbation placed at Point C in Fig. 5. (b) Perturbation placed at Point D in Fig. 5.

the symmetrical plane, the attenuation-pole frequencies are different, although coupling strength (the coupling coefficient between the orthogonal modes) is equal.

Fig. 7 shows resonance characteristics in relation to characteristic impedance ratio K_z. The line length of the perturbed portion $2\theta_p$ at resonance frequency f_r is kept at 5°. When K_z is one, the structure is a simple ring resonator and the coupling coefficient becomes zero. The coupling coefficient is identical at the two locations (Points C and D) where K_z has an inverse relationship. In a practical range of $K_z = 0.5$~2, the resonance frequencies can be considered to change linearly, thus making design far more simple. Analytical results imply that the attenuation poles are not generated when K_z is larger than one, meaning that the perturbation line is narrower than the resonator transmission line. The reason is that the magnitude of the transfer admittances of the two paths connecting the input and output (Y'_{21} and Y''_{21}) are not equal.

C. Experimental Resonance Characteristics

Several dual-mode resonators based on a microstrip-line configuration were fabricated and evaluated. RT/Duroid was chosen for the dielectric substrate, possessing a relative dielectric constant of 10.5, thickness of 1.27 mm, and loss tangent of 0.002. The conductor was copper with a thickness of 35 μm. The characteristic impedance of the ring transmission line Z_r was 50 Ω. The effective dielectric constant was estimated at 6.9 in order to determine the dimension of the ring resonator to possess an electrical length of 360° at a resonance frequency of 1.9 GHz. Perturbation was loaded at Point C. The resonator was coupled with the input and output transmission lines by a gap of 1 mm,

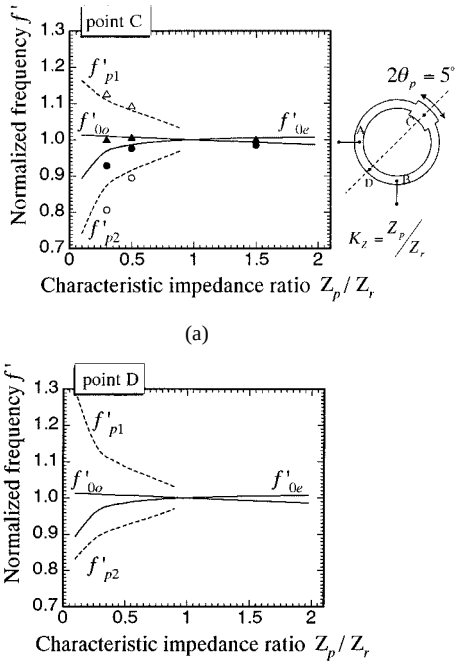

Fig. 7. Resonance characteristics of the stepped-impedance-type dual-mode ring resonator as a function of impedance ratio K_z. (a) Perturbation placed at Point C in Fig. 5. (b) Perturbation placed at Point D in Fig. 5.

creating a coupling loose enough to neglect any effects on resonance characteristics. Measured resonance characteristics for impedance ratio $K_z = 0.5$ and electrical length $2\theta_p = 20°$ are illustrated in Fig. 3, where two resonance modes with attenuation poles on both sides can be observed. Other experimental results are plotted on the analyzed results in Figs. 6 and 7, where black plots indicate the measured resonance frequencies, while white plots show the measured frequencies of attenuation poles. Results suggest a good agreement between the measured and analyzed results, while a small discrepancy can be observed for a large impedance ratio. In the tested resonators, the step in characteristic impedance was realized by changing transmission linewidth. Thus, for a large impedance ratio, the change of width becomes significant and the effects of the parasitic capacitance at the step can no longer be neglected. However, filters applied to wireless equipment usually require a relative bandwidth of less than 10%, making it unnecessary to design the perturbation large enough to exhibit such effects. Hence, the analysis method presented is sufficient for design.

III. Dual-Mode Ring Filter

A. Design

The attenuation-pole frequencies of a dual-mode ring resonator change in accordance to the structure or position of the perturbation, even when the coupling strength is kept constant. This implies that the attenuation characteristic of a filter based on this resonator structure is dependent on the perturbation structure. Thus, our discussions focus on a filter design method in which passband characteristics are regarded prior to attenuation performance, based on the conditions of a given passband bandwidth. From the conditions, the element values (g-parameters) of the Chebyshev type filter are calculated by (5) as follows:

$$\begin{aligned} g_o &= 1.0 \\ g_1 &= \frac{\sqrt{2}}{\gamma} \\ g_2 &= \frac{\sqrt{2}\gamma}{\gamma^2+1} \\ g_3 &= \coth^2\frac{\beta}{4} \end{aligned} \tag{5}$$

where

$$\begin{aligned} \beta &= \ln\left(\coth\frac{L_p}{17.37}\right) \quad (L_p\text{: passband ripple [dB]}) \\ \gamma &= \sinh\left(\frac{\beta}{4}\right). \end{aligned} \tag{6}$$

Coupling circuits applied in the design of a BPF, such as inter-stage coupling and input-and-output couplings, are discussed in the following sections.

1) Inter-Stage Coupling: The inter-stage coupling coefficient of a dual-mode filter corresponds to the coupling between the orthogonal modes of the dual-mode resonator, and is strongly dependent on the structure of the perturbation. When the element value of the filter is $g_0 \sim g_3$, the relative bandwidth is w, and the resonance frequencies of the resonator is f_{0e} and f_{0o}, the inter-stage coupling coefficient k_{12} is given by (7) as follows:

$$k_{12} = \frac{w}{\sqrt{g_1 g_2}} = \frac{2|f_{0e} - f_{0o}|}{f_{0e} + f_{0o}}. \tag{7}$$

2) Input and Output Couplings: An approximate design method is applied by assuming a two-stage BPF where capacitive coupling is adopted for input and output couplings. The coupling capacitance can be obtained by the external Q and the susceptance slope parameter of the resonator. Since the resonator and the coupled circuit cannot be divided, it is difficult to derive the slope parameter. However, when the relative bandwidth is less than 2%, the slope parameter of the ring resonator without the discontinuity can be applied approximately. The approximated slope parameter b_r is shown by (8) and the external Q Q_e is calculated by (9), then the coupling capacitance C_s is obtained by (10), where the G_s means source conductance as follows:

$$b_r \cong \frac{\pi}{Z_r} \tag{8}$$

$$Q_e = \frac{g_0 g_1}{w} \tag{9}$$

$$C_s = \frac{G_s}{\sqrt{(G_s Q_e / b_r) - 1}}. \tag{10}$$

The attenuation-pole frequencies do not change by input and output coupling circuits. Center frequency of the filter corresponds to the center of the resonance frequencies of the even and odd modes. The center frequency shift due to the inter-stage coupling is little, as shown in Fig. 6, the shift due to input and output coupling circuits yields adjustment of the physical dimension of the ring resonator. Yet as illustrated above, the structural simplicity of the dual-mode filter enables easy calculation of approximate transmission response, and by applying these

TABLE I
DESIGN PARAMETERS OF THE EXPERIMENTAL FILTERS

Filter type	i	ii	iii
Center frequency f_0	1.907GHz		
Rerative bandwidth w	0.5%	1.4%	2.0%
Length of the stepped impedance portion $2\theta_s$	8°	18°	28°
Coupling capacitance C_s	0.28pF	0.44pF	0.54pF

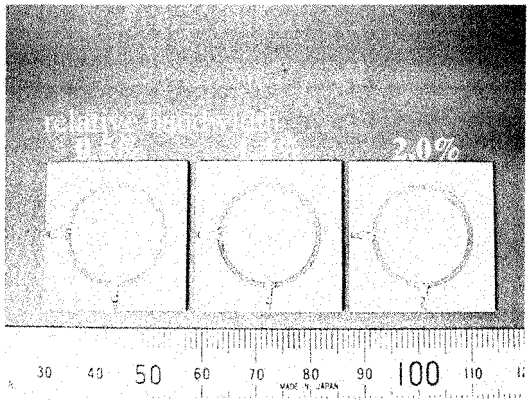

Fig. 8. Photograph of the experimental dual-mode filters.

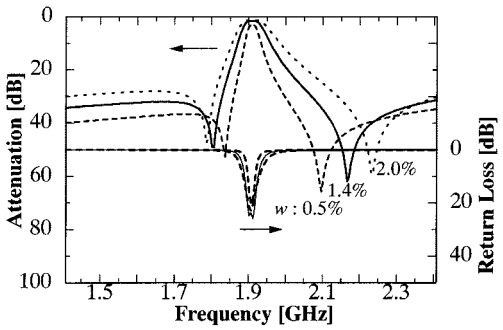

Fig. 9. Calculated responses of the experimental filters.

results as initial values, rigorous design parameters can be obtained through computer-aided design (CAD) optimization.

B. Experimental Results

Based on the above design method, three experimental dual-mode filters with a center frequency f_0 of 1.9 GHz and relative bandwidth w of 0.5%, 1.4%, and 2.0% were designed and fabricated using a copper microstrip line on the above-mentioned RT/Duroid substrate. Impedance ratio K_z was chosen as 0.8 ($Z_r = 50\ \Omega$, $Z_s = 40\ \Omega$) and the relative bandwidth was adjusted by the length of perturbation transmission line $2\theta_s$. Design parameters are summarized in Table I.

Fig. 8 shows a photograph of the experimental filters fabricated on a substrate measuring 27 mm × 27 mm. Lumped-element chip capacitors are adopted as input and output coupling capacitors. Calculated results by a general-purpose circuit simulator are illustrated in Fig. 9, while measured results are shown in Fig. 10. A good agreement is seen between design and actual results, thus demonstrating the validity of the design method described. In addition, the attenuation poles appear in both the

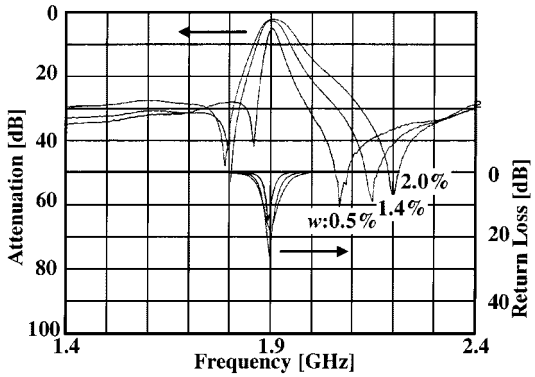

Fig. 10. Measured responses of the experimental filters.

upper and lower sides of the passband, giving a steep gradient of attenuation in spite of a two-stage BPF structure.

IV. CONCLUSION

In this paper, we have presented the analysis method for the dual-mode resonator: a ring-resonator structure possessing two ports spatially separated at 90° in electrical length, with a perturbation loaded at its symmetrical plane. Based on this method, the even- and odd-mode resonance frequencies and attenuation-pole frequencies were obtained and the resonance characteristic are clarified for a dual-mode resonator applying an impedance step as a perturbation structure. Experimental results were presented to demonstrate the validity of the analysis method. In addition, a design method was proposed for a dual-mode filter based on the dual-mode resonator. Several filters were designed and fabricated and excellent attenuation characteristics were obtained. The proposed design method is extremely effective for filter design used for wireless communication equipment.

Low radiation property is feature of the ring resonator worthy of note. Radiation loss generally shows a remarkable increase in the millimeter-wave region and, thus, it becomes difficult to adopt the half-wavelength resonator with open-circuited ends, which is conventionally used in the microwave region. In addition, the ring resonator gives more allowance to physical dimensions because of its one-wavelength resonator structure, resulting in a practical advantage of easy manufacturing. These features bring high hopes especially for the proposed filter to millimeter-wave ICs.

REFERENCES

[1] M. Makimoto and S. Yamashita, "Compact bandpass filters using stepped impedance resonators," *Proc. IEEE*, vol. 67, pp. 16–19, Jan. 1979.
[2] M. Sagawa, M. Makimoto, and S. Yamashita, "A design method of bandpass filters using dielectric-filled coaxial resonators," *IEEE Trans. Microwave Theory Tech.*, vol. MTT-33, pp. 152–157, Feb. 1985.
[3] M. Sagawa, M. Makimoto, K. Eguchi, and F. Fukushima, "Miniaturized antenna duplexers for portable radio telephone terminals," *Trans. IEICE*, vol. E-74, no. 5, pp. 1221–1225, May 1991.
[4] Y. Kobayashi and K. Kubo, "Canonical bandpass filters using dual-mode dielectric resonators," in *IEEE MTT-S Int. Microwave Symp. Dig.*, vol. D-3, June 1987, pp. 137–140.
[5] I. Awai and T. Yamashita, "A dual mode bandpass filter based on degenerate rectangular dielectric-waveguide resonator," in *Proc. Asia–Pacific Microwave Conf.*, vol. 1, Dec. 1994, pp. 75–78.

[6] R. R. Bonetti and A. E. Williams, "Quadruple mode filter," in *IEEE MTT-S Int. Microwave Symp. Dig.*, vol. D-5, June 1987, pp. 145–147.
[7] I. Wolff, "Microstrip bandpass filters using degenerate modes of a microstrip ring resonator," *Electron. Lett.*, vol. 8, no. 12, pp. 163–164, June 1972.
[8] J. A. Curtis and S. J. Fiedziuszko, "Miniature dual mode microstrip filters," in *IEEE MTT-S Int. Microwave Symp. Dig.*, 1991, pp. 443–446.
[9] U. Karacaoglu, I. D. Robertson, and M. Guglielmi, "An improved dual-mode microstrip ring resonator filter with simple geometry," in *Proc. 24th European Microwave Conf.*, Sept. 1994, pp. 472–477.
[10] H. Yabuki, M. Sagawa, M. Matsuo, and M. Makimoto, "Stripline dual-mode ring resonators and their application to microwave devices," *IEEE Trans. Microwave Theory Tech.*, vol. 44, pp. 723–729, May 1996.
[11] M. Matsuo, H. Yabuki, M. Sagawa, and M. Makimoto, "Fundamental characteristics of the coupling between the orthogonal resonant modes in a ring resonator," IEICE, Tokyo, Japan, Tech. Rep. MW95-101, Nov. 1995.

Michiaki Matsuo was born in Japan, in 1967. He received the B.S. and M.S. degrees in electrical engineering from Waseda University, Tokyo, Japan, in 1990 and 1992, respectively.

In 1992, he joined the Matsushita Electric Industrial Corporation Ltd., Kawasaki, Japan, where he performed research and development work on microwave components, in particular, resonators and filters. In 1996, he was transferred to the Matsushita Research Institute Tokyo Inc., Kawasaki, Japan, where he has been engaged in development of microwave equipment for advanced mobile communication systems.

Mr. Matsuo is a member of the Institute of Electronics, Information and Communication Engineers (IEICE), Japan.

Hiroyuki Yabuki was born in Japan, in 1961. He received the B.S. and Dr.Eng. degrees in electrical engineering from Keio University, Yokohama, Japan, in 1984 and 2000, respectively.

In 1984, he joined the Matsushita Research Institute Tokyo Inc., Kawasaki, Japan, where he performed research and development work on UHF radio circuits for mobile communication systems, and is currently concerned with microwave and millimeter-wave ICs and component. He is also engaged in research and development of radio equipment for advanced mobile communication systems.

Dr. Yabuki is a member of the Institute of Electronics, Information and Communication Engineers (IEICE), Japan.

Mitsuo Makimoto (M'88–SM'97) was born in Japan, in 1944. He received the B.S. and M.S. degrees in electrical engineering from Yokohama National University, Yokohama, Japan, in 1968 and 1970, respectively, and the Dr.Eng. degree from the Tokyo Institute of Technology, Tokyo, Japan, in 1990.

In 1970, he joined the Matsushita Research Institute Tokyo Inc., Kawasaki, Japan, where he performed research and development work on microwave ICs and components for radio communication systems. He is currently a director of Mobile Communication Research Laboratory, Matsushita Research Institute Tokyo Inc., where he is engaged in research on microwave devices and antenna and wireless networks for advanced mobile communication systems.

Dr. Makimoto is a member of the Institute of Electronics, Information and Communication Engineers (IEICE), Japan and the Institute of Image Information and Television Engineers of Japan (ITE).